Acta Oceanol. Sin., 2019, Vol. 38, No. 1, P. 5–12
https://doi.org/10.1007/s13131-019-1366-x
http://www.hyxb.org.cn
E-mail: hyxbe@263.net

Seasonal prediction skills of FIO-ESM for North Pacific sea surface temperature and precipitation

Yiding Zhao[1, 2], Xunqiang Yin[2, 3, 4], Yajuan Song[2, 3, 4], Fangli Qiao[2, 3, 4*]

[1] College of Oceanic and Atmospheric Sciences, Ocean University of China, Qingdao 266100, China

[2] First Institute of Oceanography, Ministry of Natural Resources, Qingdao 266061, China

[3] Laboratory for Regional Oceanography and Numerical Modeling, Pilot National Laboratory for Marine Science and Technology (Qingdao), Qingdao 266071, China

[4] Key Laboratory of Marine Science and Numerical Modeling, Ministry of Natural Resources, Qingdao 266061, China

Received 10 September 2017; accepted 6 February 2018

Abstract

The seasonal prediction of sea surface temperature (SST) and precipitation in the North Pacific based on the hindcast results of The First Institute of Oceanography Earth System Model (FIO-ESM) is assessed in this study. The Ensemble Adjusted Kalman Filter assimilation scheme is used to generate initial conditions, which are shown to be reliable by comparison with the observations. Based on this comparison, we analyze the FIO-ESM 6-month hindcast results starting from each month of 1993–2013. The model exhibits high SST prediction skills over most of the North Pacific for two seasons in advance. Furthermore, it remains skillful at long lead times for mid-latitudes. The reliable prediction of SST can transfer fairly well to precipitation prediction via air-sea interactions. The average skill of the North Pacific variability (NPV) index from 1 to 6 months lead is as high as 0.72 (0.55) when El Niño-Southern Oscillation and NPV are in phase (out of phase) at initial conditions. The prediction skill of the NPV index of FIO-ESM is improved by 11.6% (23.6%) over the Climate Forecast System, Version 2. For seasonal dependence, the skill of FIO-ESM is higher than the skill of persistence prediction in the later period of prediction.

Key words: seasonal prediction, North Pacific, sea surface temperature, precipitation, FIO-ESM climate model

Citation: Zhao Yiding, Yin Xunqiang, Song Yajuan, Qiao Fangli. 2019. Seasonal prediction skills of FIO-ESM for North Pacific sea surface temperature and precipitation. Acta Oceanologica Sinica, 38(1): 5–12, doi: 10.1007/s13131-019-1366-x

1 Introduction

The North Pacific climate variability significantly affects the physical, biological and human environment over the ocean and its adjacent continents (Latif and Barnett, 1994; Mantua et al., 1997; Overland et al., 2010). Accurate predictions of climate variability are crucial for social management, such as for disaster prevention in the affected regions. The temporal characteristics of the North Pacific sea surface temperature (SST) exhibit variability on different time scales extending from weather forecasting scale to decadal or even longer scales. On the interannual and interdecadal time scales, the North Pacific SST can strongly influence the El Niño-Southern Oscillation (ENSO) and the tropical Pacific physical variabilities (Wang et al., 2009; Di Lorenzo et al., 2010; Yeh et al., 2015; Yu et al., 2017). In addition to its influences on the tropical ocean, the evolution of the North Pacific SST modulates the weather and climate over North America and East Asia on the seasonal time scale (Lau et al., 2004; Zhou et al., 2007; Hu and Huang, 2009; Beattie and Elsberry, 2012; Li et al., 2017). Besides, ocean environmental prediction in the North Pacific region, with an emphasis on the mid-latitudes, is the focus of the North Pacific Marine Science Organization (PICES, http://meetings.pices.int/). Therefore, accurate prediction of the seasonal variability in the North Pacific region is an important issue in climate research.

Studies have generally focused on seasonal prediction in the tropical Pacific, but prediction in the extra-tropics has received less attention. In these limited studies, various methods and models have been used to predict the North Pacific SST and precipitation with short lead times. On seasonal and longer time scales, based on whether linear method (Landman and Mason, 2001; Alexander et al., 2008) or two-tier method (Auad et al., 2004), the SST prediction skills were limited at mid-latitudes of the North Pacific. Such limitation should be attributed to the lack of proper physical processes and air-sea interactions. Therefore,

Foundation item: The National Natural Science Foundation of China (NSFC)-Shandong Joint Fund for Marine Science Research Centers under contract No. U1606405; the National Programme on Global Change and Air-Sea Interaction under contract Nos GASI-IPOVAI-05 and GASI-IPOVAI-06; the International Cooperation Project on the China-Australia Research Centre for Maritime Engineering of Ministry of Science and Technology, China under contract No. 2016YFE0101400; the Qingdao National Laboratory for Marine Science and Technology through the AoShan Talents Program under contract No. 2015ASTP; the Transparency Program of Pacific Ocean-South China Sea-Indian Ocean under contract No. 2015ASKJ01; the Scientific and Technological Innovation Project of Qingdao National Laboratory for Marine Science and Technology under contract No. 2016ASKJ16; the Public Science and Technology Research Funds Projects of Ocean under contract No. 201505013; the China-Korea Cooperation Project on the Trend of North-West Pacific Climate Change.

*Corresponding author, E-mail: qiaofl@fio.org.cn

coupled climate model was expected to improve seasonal, interannual and decadal prediction. Lienert (2011) studied seasonal prediction skill based on coupled climate data assimilation and prediction system (CHFP2). This system reasonably predicted the historical evolution of the Pacific decadal oscillation (PDO) on seasonal time scale. Wen et al. (2012) investigated the skill of the North Pacific SST with the National Centers for Environmental Prediction (NCEP) Climate Forecast System (CFS). They demonstrated that the North Pacific SST, except for the Kuroshio-Oyashia Extension (KOE) region, could be predicted with reasonable skill for two-season lead times. Hu et al. (2014) examined the prediction skill of North Pacific variability (NPV) in a fully coupled forecast system (NCEP CFSv2). The model and data assimilation improvements of CFSv2 resulted in higher skill in the North Pacific. Although these coupled climate models have shown some capabilities of predicting the North Pacific climate variability, the prediction skills at mid-latitudes are still relatively low.

The prediction skill for the mid-latitudes of the North Pacific is constrained by the chaotic and unpredictable nature of the atmospheric circulation. The predictability in the North Pacific is overall much lower than that in the tropical ocean due to the small signal-to-noise ratio (Goddard, 2012). Thus, accurate prediction of the North Pacific SST at mid-latitudes has been a long-standing challenge. Comparatively, precipitation processes and patterns have much smaller spatial scales and are more affected by local scale features (Goddard, 2012). Coupled climate models presently experience greater difficulty simulating the regional patterns and temporal variations of precipitation (Dai, 2006; Xing et al., 2016).

To extend skillful mid-latitude predictions to longer times, the physical processes of the model, initialization procedures and the quantity of ocean observations require further improvement. Although Hasselmann (1991) noted that the ocean surface wave plays an important role in the earth climate system, and that this process should be well considered in the climate model, the inclusion of the surface wave into ocean general circulation models, climate models and earth system models remains challenging. The First Institute of Oceanography Earth System Model (FIO-ESM) is the first climate model coupled with the surface-wave component proposed by Qiao et al. (2013) to conquer this challenge. Numerical experiments have shown that the additional wave-induced vertical mixing significantly improves the simulation of the North Pacific SST when compared with model runs without wave effects (Song et al., 2007).

In addition to the physical processes, the initial conditions and ensemble methods are also important for seasonal prediction. The greater availability of ocean observations has promoted the development and application of ocean data assimilation. The effective use of these observations for data assimilation is important in ocean data assimilation research (Haines, 1991; Ezer and Mellor, 1994, 1997; Yin et al., 2010; Ratheesh et al., 2012). The data assimilation scheme Ensemble Adjusted Kalman Filter (EAKF) (Anderson, 2001) was introduced into the FIO-ESM (Yin, 2015). The results indicated many improvements, not only in the upper ocean, but also in atmospheric motions, vapor distribution (Chen et al., 2015) and sea ice evolution (Shu et al., 2015). This data assimilation scheme has been used in climate prediction for 2015/2016 El Niño events and showed the potential to enhance ENSO prediction skill (Song et al., 2015). The improved ENSO prediction could further enhance NPV prediction since the NPV is highly correlated with the variability of ENSO due to the atmospheric bridge mechanism (Lau and Nath, 1994, 1996; Alexander et al., 2002).

In this study, we quantify the FIO-ESM's prediction skills for SST and precipitation in the North Pacific. This paper is organized as follows: Section 2 briefly describes the data and methods used in this study, Section 3 assesses the data assimilation and hindcast results of the FIO-ESM, and Section 4 summarizes the major results.

2 Data and methods

2.1 *Data assimilation and hindcast data from FIO-ESM*

Based on the non-breaking wave-induced mixing theory proposed by Yuan et al. (1999) and Qiao et al. (2004, 2010), a coupled climate model including the surface wave was developed and named FIO-ESM (Qiao et al., 2013), which was the first attempt to couple with the surface-wave model. The FIO-ESM includes five model components: the atmospheric component CAM3.0 (Community Atmosphere Model Version 3.0), the land component CLM3.5 (Community Land Model Version 3.5), the sea-ice component CICE4 (Los Alamos Sea Ice Model Version 4.0), the ocean circulation component POP2.0 (Parallel Ocean Program Version 2.0), and the wave component developed by the Key Lab of Marine Science and Numerical Modeling (MASNUM), Ministry of Natural Resources of China. In this study, only the data from the atmospheric and oceanic components are analyzed. The horizontal resolution of the atmospheric model is T42 (about 2.875°) with 26 vertical layers. The horizontal resolution of the ocean circulation model is 1.1°×0.3° to 1.1°×0.5° with 40 vertical layers. The EAKF scheme has been used to establish a data assimilation system for the FIO-ESM (Chen et al., 2015; Yin, 2015) in which the model runs with 10 ensemble members. The SST and SLA (sea level anomaly) data from satellite observations are assimilated into the FIO-ESM. A long-term data assimilation experiment is conducted that covers all calendar months from 1992 to 2013. With the assimilation data as the initial conditions, Song et al. (2015) carried out a series of 6-month El Niño hindcast experiments from 1993 to 2013 as a test. The monthly data assimilation results and hindcast results of the FIO-ESM from 1993 to 2013 are used in this study. To quantify the influence of the initial conditions used for prediction, the simulation capability of the FIO-ESM is examined before the analysis of the seasonal prediction skill based on the hindcast results.

2.2 *Data for validation*

The SST data used in this paper are daily-averaged Advanced Very High Resolution Radiometer (AVHRR) satellite observation data with a horizontal resolution of (1/4)°×(1/4)°. Since the observation data include signals of mesoscale process due to their high horizontal resolution, a 1.5° running mean average is conducted, and the daily SST is then averaged into a monthly mean.

The precipitation data used in this paper are provided by the Global Precipitation Climatology Project (GPCP). These data are a product of the World Climate Research Program (WCRP), which combines infrared and microwave satellite observations and global monthly precipitation data generated by more than 6 000 conventional precipitation observations. The horizontal resolution of GPCP is 2.5°×2.5°.

2.3 *Methods*

For simplicity, the average of the 10 ensemble members is used in this study. Before verification, SST data from the FIO-ESM and from the AVHRR are both interpolated onto the grid of 1°×1°. The precipitation data of FIO-ESM are interpolated onto

the GPCP grid. Both the simulated and observed SST anomalies (SSTAs) are calculated with respect to each monthly climatology, and the predicted SSTAs are calculated in the same way according to their own time series of different lead times. The SSTAs are then converted into 3-month means. The following evaluation criteria are used to calculate the fidelity of the model data.

(1) Root mean square error

The root mean square error (RMSE), which gives an estimate of the deviation of the simulated value relative to the observational value, is used to assess the error distribution of the data assimilation results. At a certain grid point, it is the square root of the mean of the squared differences between the corresponding elements of the model and the observations. The equation for RMSE is:

$$\mathrm{RMSE} = \sqrt{\frac{1}{T}\sum_{t=1}^{T}(S_t - O_t)^2}, \qquad (1)$$

where S represents the simulation at each spatial grid point; O represents the observational value at the corresponding grid point; and T represents the length of the time series.

(2) Anomaly correlation coefficient

The prediction skill for SST and precipitation is quantified by the anomaly correlation coefficient (ACC), which is a commonly used measure of the linear relationship between the predicted anomalies and the observed anomalies. The equation for ACC is:

$$\mathrm{ACC} = \frac{\mathrm{cov}(S,O)}{\sigma_S\sigma_O} = \frac{1}{T}\sum_{t=1}^{T}(S_t - \overline{S_t})(O_t - \overline{O_t})/\sigma_S\sigma_O, \qquad (2)$$

where cov(S, O) represents the covariance of the predicted and observational anomaly; σ represents the standard deviation of the variable; and the overbar indicates the temporal average of the time series.

(3) NPV index

The NPV index, defined as the SSTAs averaged in 30°–50°N and 150°E–150°W, is used to test the prediction skills. Previous studies (Hu et al., 2014; Duan and Wu, 2015) showed that the NPV index has a strong negative correlation with the PDO index (Mantua et al., 1997) and can well represent the total SST variance in the North Pacific. As the NPV index is a typical index that reflects the temporal evolution of the North Pacific SST, it is popularly used to study the North Pacific climate variability.

3 Results and discussion

3.1 *Data assimilation results*

The SST and precipitation are two key indicators of climate variability, and their seasonal variations have received wide attention. This study will focuses on these two variables in the North Pacific. To examine whether the data assimilation results can provide reliable initial conditions for prediction, we first assess the SST and precipitation simulation capabilities after assimilation.

The average of the SSTAs in the North Pacific is calculated. Figure 1 shows the interannual variability of the spatial mean SSTAs in the North Pacific. The data assimilation results and the observations have a strong correlation (ACC, 0.92; RMSE, 0.058°C), which indicates that the temporal evolution of SST is reliable in the North Pacific. For the spatial distribution of RMSE (Fig. 2), the largest RMSE (0.3–0.5°C) occurs near the KOE region and off the

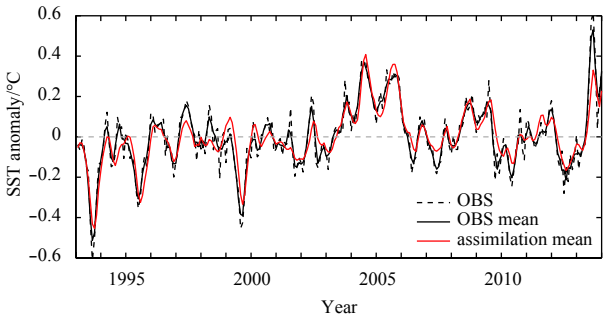

Fig. 1. Time series of 3-month mean SSTAs with respect to 1993–2013 climatology for the North Pacific region (30°–65°N, 110°E–100°W). Black and red lines represent SSTAs from the observation data and the FIO-ESM assimilation result, respectively. Dashed gray line represents SSTAs from the observation without 3-month mean.

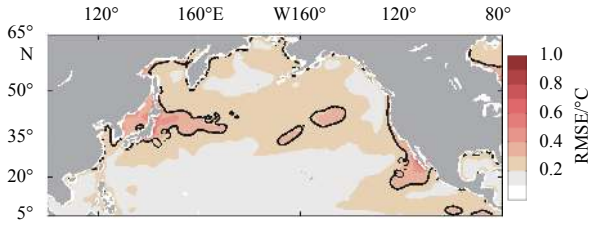

Fig. 2. RMSE distribution of SSTAs in the North Pacific. Only the 0.3 contour is plotted.

California coast. The KOE region is characterized by complex interactions between dynamics and thermodynamics and between atmosphere and ocean (Kelly et al., 2010), which is difficult to simulate in a coupled system. Most climate models with coarse resolution are not able to resolve the dynamics necessary for the correct location or strength of the KOE (Kwon et al., 2010). The bias off the coast of California presenting in most coupled models is generally associated with the atmospheric general circulation model's lack of ability to generate marine stratocumulus clouds in this anticyclonic region (Guilyardi and Madec, 1997). In general, the RMSE in most regions of the North Pacific is less than 0.3°C. The simulated SST is basically consistent with the observation.

The ability of the model to simulate precipitation is also examined. The comparison between the climatological precipitation and the observations is shown in Fig. 3. The pattern of precipitation is consistent with the observations, with more precipitation in the tropical and westerly zone and less in the subtropical high region. The mean error is less than 1 mm/d. In the FIO-ESM, the atmospheric component has not been assimilated, and only the SST and SLA are assimilated into the ocean general circulation model. Improvements in the ocean simulation can affect the low-level atmospheric heat transport and movement process via air-sea interactions, which makes the atmospheric humidity and cloud cover more realistic (Chen et al., 2015). Thus, the simulation abilities of the oceanic and atmospheric components are both improved.

The results above show the capability of FIO-ESM to represent SST and precipitation in the North Pacific. Thus, the data assimilation results should be reasonable to provide the initial conditions for further prediction.

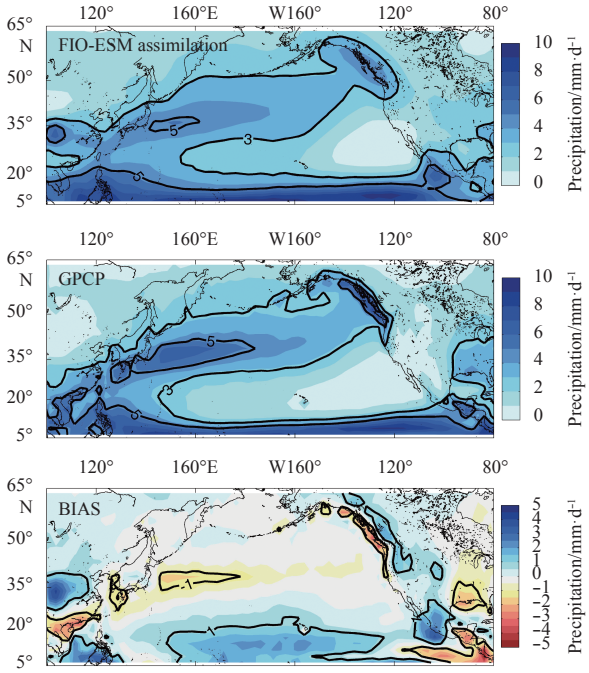

Fig. 3. Distributions of long-time averaged precipitation and its deviations in the North Pacific. Upper panel is the FIO-ESM assimilation result. Middle panel is the GPCP result. Bottom panel is the difference between the FIO-ESM and GPCP results.

3.2 *Seasonal prediction skill*

Based on the initial conditions, a series of 6-month hindcasts are conducted for each month from 1993 to 2013. We analyze the hindcast results of FIO-ESM and examine the performance of the model in predicting the North Pacific SST and precipitation. First, we assess the prediction skill of seasonal anomalies and then assess seasonal prediction skill of NPV, including its interannual variability and seasonal dependence.

The evolution of the ACC of the North Pacific SST is shown in Fig. 4. The ACC of the SST first decays near the KOE region, followed by the California coast and the western tropical Pacific, resulting in higher skill in the eastern North Pacific than in the western North Pacific. The model exhibits high SST prediction skills over most of the North Pacific for two seasons in advance and remains skillful at long lead times for mid-latitudes. Compared with previous studies based on the coupled climate models (Lienert, 2011; Wen et al., 2012; Hu et al., 2014; Zhu et al., 2015), FIO-ESM shows higher seasonal prediction skill for the North Pacific SST. We take the hindcast results of NCEP CFSv2 as an example. NCEP CFSv2 is an upgraded version of CFSv1 and has reasonable prediction skill for SSTAs in the North Pacific (Hu et al., 2014). The SST prediction skill of the FIO-ESM and CFSv2 shows a similar distribution and evolution of the decaying process, while the FIO-ESM shows higher skills at all lead times, especially at mid-latitudes (Fig. 4). The simulation of SST is indeed effectively improved to the north of 35°N in the North Pacific by consideration of wave-induced mixing (Song et al., 2007), so the improvement of the SST prediction skill at mid-latitudes could be due to the inclusion of the surface-wave component in the FIO-ESM.

As discussed above, the FIO-ESM makes more precise predictions for the North Pacific SST. The accuracy of SST plays an important role in improving precipitation in the climate system, which makes water distribution more reasonable (Chen et al., 2015; Yin, 2015). Next, we analyze the prediction skill for North Pacific precipitation.

The ACCs for North Pacific precipitation in summer (JJA) and winter (DJF) are calculated (Fig. 5). The initial months and target prediction months in our numerical experiment are the same as those in CFSv2 (Zhang et al., 2017; Kim et al., 2012). For summer prediction, the FIO-ESM hindcast is initialized on April 1 during 1993–2013. Skillful precipitation predictions mostly reside in the tropical oceans. Over the mid-latitudes, there are some regions

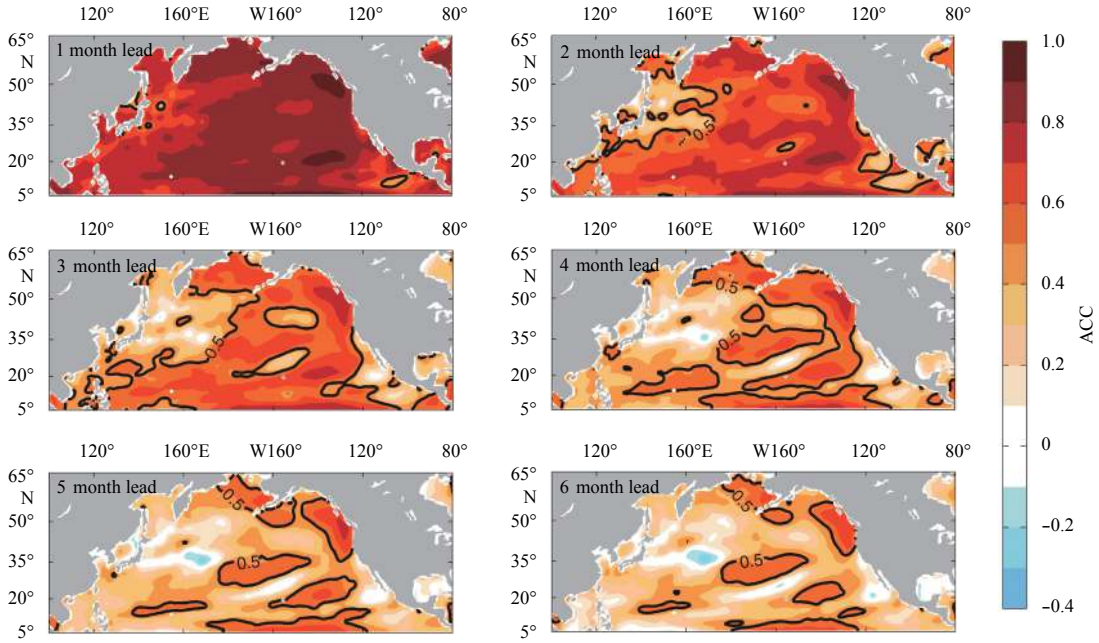

Fig. 4. Distributions of SST ACC between the FIO-ESM hindcast and the observation in the North Pacific for 1 to 6 months lead. Only the 0.5 contours are plotted.

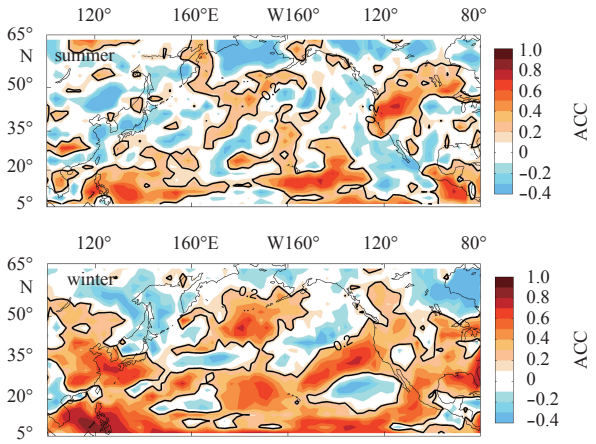

Fig. 5. Distributions of precipitation ACC between the FIO-ESM hindcast and GPCP in the North Pacific. Upper panel is the skill for summer (JJA) precipitation and bottom panel is the skill for winter (DJF) precipitation. Only the 0.2 contours are plotted.

with systematic skill, such as the central North Pacific and North America. For winter prediction, the FIO-ESM hindcast is initialized on November 1 during 1993–2013. It is evident that the skill for winter precipitation is higher than that for summer. The FIO-ESM shows high skills at mid-latitudes. Even at 50°N, the ACC can still reach 0.2. The distribution of skillful regions in the FIO-ESM is similar to that in CFSv2. Compared with CFSv2, the FIO-ESM shows significant improvement at mid-latitudes, which likely corresponds to the improvement in local SST prediction. Even without assimilation of the atmospheric component in the FIO-ESM, the prediction skill for North Pacific precipitation is comparable to that of CFSv2. Therefore, we suggest that better SST prediction in the FIO-ESM can transfer fairly well to precipitation prediction via air-sea interactions.

3.3 *NPV prediction*

The variability in the North Pacific is well represented by the NPV index. We calculate the NPV index as the evaluation criteria for seasonal prediction and quantify the improvement of prediction skill at mid-latitudes.

Figure 6 shows the FIO-ESM's ability to predict the monthly variability of the NPV index. Although there exist some drifts, the 6-month hindcasts (red lines) can basically catch the observation variability (black line). The development of cold and warm events in the North Pacific also can be reflected. It is notable that the NPV index exhibits different skills in different time periods, which shows interannual and seasonal dependence.

We first assess the prediction skill of the NPV on the interannual time scale. The phase relationship between the ENSO and NPV at initial conditions affects the prediction skill for the NPV index. Skillful prediction of NPV mainly results from the impact of ENSO teleconnection to the cases of an in-phase relation. Opposite phase variations imply that part of the NPV is not forced by ENSO, but its local variability influenced by air-sea interactions (Hu et al., 2014). We calculate the ACCs of the NPV index when ENSO and NPV are in phase and out of phase separately at initial conditions, following the approach of Hu et al. (2014). The ACCs of the NPV index are shown in Fig. 7. The average skill from 1 to 6 month lead is as high as 0.72 (0.55) in the in-phase (out-of-phase) cases. The differences between the two cases reach a maximum at 4 month lead, which implies that it takes 4 months

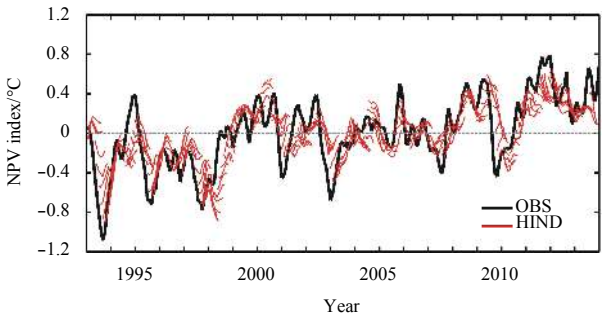

Fig. 6. Monthly variability of the FIO-ESM predicted NPV index. Black line is calculated from the observation data. Red lines are 6-month hindcasts that started every month.

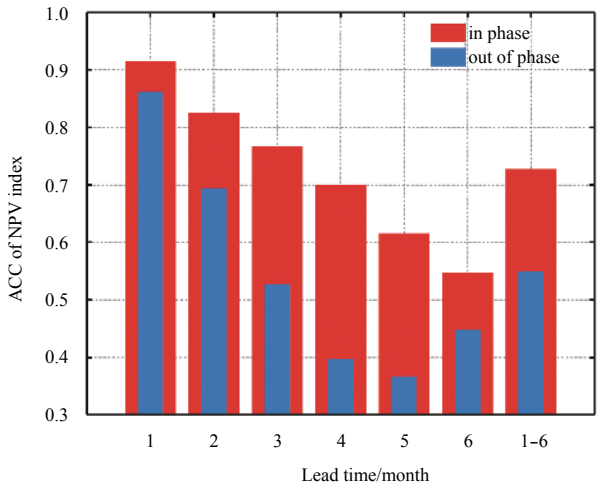

Fig. 7. Dependence of prediction skills (ACC) for the FIO-ESM predicted NPV index on lead time and phase relationship. Red and blue bars represent the prediction skills of the NPV index for in-phase and out-of-phase variations between the Niño 3.4 index and the NPV index at initial conditions. The rightmost bar is the average skill from 1 to 6 months lead.

for the ENSO-NPV phase relation to affect the prediction skill for the NPV index. When ENSO and NPV are in phase at initial conditions, the ACCs of the NPV index in the FIO-ESM are statistically higher than that in CFSv2 by 0.12, 0.12, 0.12, 0.08, 0.03 and 0.01 for lead times from 1 to 6 months, respectively. When ENSO and NPV are out of phase, the ACCs are higher than that in CFSv2 by 0.16, 0.20, 0.14, 0.04, 0.01 and 0.09, respectively. It indicates that FIO-ESM has a significant advantage in the first three lead months, while the skills in the last three lead months decay rapidly to a normal level. It should be the consequence of the better initial conditions achieved by the joint effects of the surface wave and the EAKF assimilation scheme. Overall, the FIO-ESM's prediction skill for the NPV index increases by 11.6% (23.6%) over the CFSv2 when ENSO and NPV are in phase (out of phase) at initial conditions. More skillful NPV index prediction to the cases of an out-of-phase relation demonstrates that the FIO-ESM exhibits a greater degree of improvement in predicting the local variability within the North Pacific.

The seasonal dependence of skill for the NPV index is further assessed (Fig. 8), which shows the ACCs as a function of target month and length of the hindcast. We compare the FIO-ESM prediction of the NPV index with persistence prediction. Both FIO-

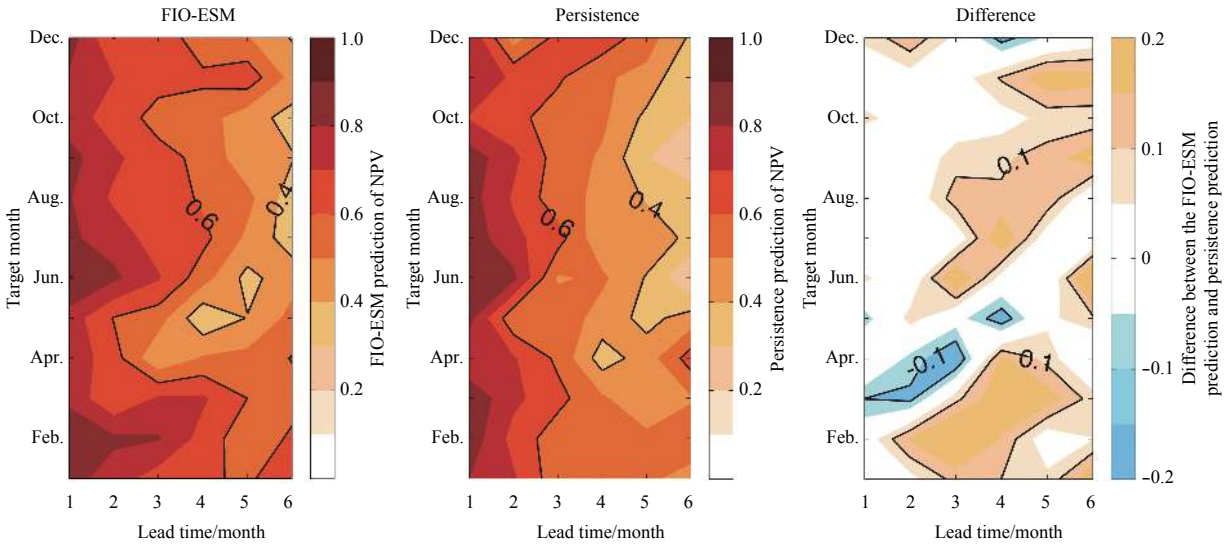

Fig. 8. Seasonal dependence of skill (ACC) for NPV as a function of target month and length of the hindcast.

ESM prediction and persistence prediction show marked seasonal variation. In particular, the NPV index has the lowest persistence in summer (i.e., the ACC falls below 0.4 after 6 months) compared with the other seasons, which also presents in the FIO-ESM prediction. It is caused by the "summer persistence barrier" (Namias and Born, 1970; Zhao et al., 2012; Duan and Wu, 2015). In winter, SSTAs extend down to the deep winter mixed layer and then become sequestered beneath the shallow summer mixed layer, which are decoupled from the surface layer. The shallow mixed layer reduces the memory of the atmosphere-ocean coupled system. Thus, winter SSTAs do not persist through the following summer. Analyzing their difference in skill, the skill of the FIO-ESM is higher than that of persistence prediction in the later period of prediction, especially in summer and winter. The higher prediction skill of FIO-ESM shows the capability of representing the oceanic dynamic and coupled processes related to NPV.

4 Summary

In this study, data assimilation and hindcast results from the FIO-ESM are assessed in the North Pacific. We aim to analyze the seasonal prediction skills of the FIO-ESM, which is coupled with a surface-wave model and uses the EAKF assimilation scheme.

Seasonal predictions depend more on the oceanic initial conditions. Due to the ocean data assimilation of the EAKF scheme, the simulation of the North Pacific SST is fairly accurate. Surface wave can improve the simulation of heat content in the upper ocean. The prediction of precipitation is subsequently improved due to the air-sea interaction. Capable of representing SST and precipitation in the North Pacific, the data assimilation results of the FIO-ESM can be reasonably used as the initial conditions for short-term climate prediction.

On this basis, we analyze the 6 months hindcast results of the FIO-ESM in 1993–2013. The FIO-ESM exhibits high SST skill over most of the North Pacific for two seasons in advance and remains skillful at long lead times at mid-latitudes. Reliable prediction of SST can transfer fairly well to the prediction of precipitation, contributing to high precipitation skills at mid-latitudes. We then assess the NPV prediction. The average skill for the NPV index from 1 to 6 months lead is as high as 0.72 (0.55) when ENSO and NPV are in phase (out of phase) at initial conditions. The FIO-ESM prediction and persistence prediction of the NPV index show similar seasonal dependence, with the lowest skill in summer, and the FIO-ESM prediction outperforms persistence prediction in the later period of prediction. The prediction skill of the FIO-ESM are compared with that of CFSv2. The FIO-ESM's prediction skill for the NPV index is higher than that of CFSv2 by 11.6% (23.6%) when ENSO and NPV are in phase (out of phase) at initial conditions.

All mentioned above suggest that the FIO-ESM has high capabilities of predicting SST and precipitation in the North Pacific. It can be applied to the operational seasonal forecast to predict the states of the North Pacific for two seasons in advance. The FIO-ESM can effectively improve the prediction skill by including both surface wave and EAKF assimilation scheme. For seasonal prediction, the mixed layer depth dominates the memory of the atmosphere-ocean coupled system. The temperature structure in the upper ocean plays an important role in the persistence of SSTA. Considering the mixing process of surface waves, the upper ocean temperature structure of ocean circulation models and climate models can be dramatically improved (Qiao et al., 2004, 2010, 2013; Huang et al., 2011, 2012). An effective assimilation scheme is also helpful to obtain a more realistic upper ocean state. Further research is still required to quantitatively investigate the relative contributions of EAKF ocean data assimilation and the inclusion of the surface-wave for the improvements of the FIO-ESM prediction skill. In addition, to upgrade the prediction system, the model resolution needs to be increased. More ensemble members and assimilation of profile data would also benefit the model's performance. These works will be carried out in the future step by step.

References

Alexander M A, Bladé I, Newman M, et al. 2002. The atmospheric bridge: The influence of ENSO teleconnections on air-sea interaction over the global oceans. Journal of Climate, 15(16): 2205–2231, doi: 10.1175/1520-0442(2002)015<2205:TABTIO>2.0.CO;2

Alexander M A, Matrosova L, Penland C, et al. 2008. Forecasting Pacific SSTs: Linear inverse model predictions of the PDO. Journal of Climate, 21(2): 385–402, doi: 10.1175/2007JCLI1849.1

Anderson J L. 2001. An ensemble adjustment Kalman filter for data assimilation. Monthly Weather Review, 129(12): 2884–2903, doi: 10.1175/1520-0493(2001)129<2884:AEAKFF>2.0.CO;2

Auad G, Miller A J, Roads J O. 2004. Pacific ocean forecasts. Journal of Marine Systems, 45(1–2): 75–90, doi: 10.1016/j.jmarsys.2003.11.010

Beattie J C, Elsberry R L. 2012. Western North Pacific monsoon depression formation. Weather and Forecasting, 27(6): 1413–1432, doi: 10.1175/WAF-D-11-00094.1

Chen Hui, Yin Xunqiang, Song Zhengya, et al. 2015. The impacts of ocean data assimilation on tropical precipitation bias in a climate model. Haiyang Xuebao (in Chinese), 37(7): 41–53

Dai Aiguo. 2006. Precipitation characteristics in eighteen coupled climate models. Journal of Climate, 19(18): 4605–4630, doi: 10.1175/JCLI3884.1

Di Lorenzo E, Cobb K M, Furtado J C, et al. 2010. Central pacific El Niño and decadal climate change in the North Pacific Ocean. Nature Geoscience, 3(11): 762–765, doi: 10.1038/ngeo984

Duan Wansuo, Wu Yujie. 2015. Season-dependent predictability and error growth dynamics of Pacific Decadal Oscillation-related sea surface temperature anomalies. Climate Dynamics, 44(3–4): 1053–1072, doi: 10.1007/s00382-014-2364-5

Ezer T, Mellor G L. 1994. Continuous assimilation of geosat altimeter data into a three-dimensional primitive equation Gulf Stream model. Journal of Physical Oceanography, 24(4): 832–847, doi: 10.1175/1520-0485(1994)024<0832:CAOGAD>2.0.CO;2

Ezer T, Mellor G L. 1997. Simulations of the Atlantic ocean with a free surface sigma coordinate ocean model. Journal of Geophysical Research: Oceans, 102(C7): 15647–15657, doi: 10.1029/97JC00984

Goddard L. 2012. Climate predictions, seasonal-to-decadal. In: Rasch P, ed. Climate Change Modeling Methodology. New York: Springer, 261

Guilyardi E, Madec G. 1997. Performance of the OPA/ARPEGE-T21 global ocean-atmosphere coupled model. Climate Dynamics, 13(2): 149–165, doi: 10.1007/s003820050157

Haines K. 1991. A direct method for assimilating sea surface height data into ocean models with adjustments to the deep circulation. Journal of Physical Oceanography, 21(6): 843–868, doi: 10.1175/1520-0485(1991)021<0843:ADMFAS>2.0.CO;2

Hasselmann K. 1991. Ocean circulation and climate change. Tellus A: Dynamic Meteorology and Oceanography, 43(4): 82–103, doi: 10.3402/tellusa.v43i4.11939

Hu Zengzhen, Huang Bohua. 2009. Interferential impact of ENSO and PDO on dry and wet conditions in the U. S. Great Plains. Journal of Climate, 22(22): 6047–6065, doi: 10.1175/2009JCLI2798.1

Hu Zengzhen, Kumar A, Huang Bohua, et al. 2014. Prediction skill of North Pacific variability in NCEP Climate Forecast System Version 2: Impact of ENSO and beyond. Journal of Climate, 27(11): 4263–4272, doi: 10.1175/JCLI-D-13-00633.1

Huang Chuanjiang, Qiao Fangli, Shu Qi, et al. 2012. Evaluating austral summer mixed-layer response to surface wave-induced mixing in the Southern Ocean. Journal of Geophysical Research: Oceans, 117(C11): C00J18

Huang Chuanjiang, Qiao Fangli, Song Zhenya, et al. 2011. Improving simulations of the upper ocean by inclusion of surface waves in the Mellor-Yamada turbulence scheme. Journal of Geophysical Research: Oceans, 116(C1): C01007

Kelly K A, Small R J, Samelson R M, et al. 2010. Western boundary currents and frontal air-sea interaction: gulf stream and Kuroshio Extension. Journal of Climate, 23(21): 5644–5667, doi: 10.1175/2010JCLI3346.1

Kim H M, Webster P J, Curry J A. 2012. Seasonal prediction skill of ECMWF System 4 and NCEP CFSv2 retrospective forecast for the Northern Hemisphere Winter. Climate Dynamics, 39(12): 2957–2973, doi: 10.1007/s00382-012-1364-6

Kwon Y O, Alexander M A, Bond N A, et al. 2010. Role of the Gulf Stream and Kuroshio-Oyashio systems in large-scale atmosphere-ocean interaction: a review. Journal of Climate, 23(12): 3249–3281, doi: 10.1175/2010JCLI3343.1

Landman W A, Mason S J. 2001. Forecasts of near-global sea surface temperatures using canonical correlation analysis. Journal of Climate, 14(18): 3819–3833, doi: 10.1175/1520-0442(2001)014<3819:FONGSS>2.0.CO;2

Latif M, Barnett T P. 1994. Causes of decadal climate variability over the North Pacific and North America. Science, 266(5185): 634–637, doi: 10.1126/science.266.5185.634

Lau K M, Lee J Y, Kim K M, et al. 2004. The North Pacific as a regulator of summertime climate over Eurasia and North America. Journal of Climate, 17(4): 819–833, doi: 10.1175/1520-0442(2004)017<0819:TNPAAR>2.0.CO;2

Lau N C, Nath M J. 1994. A modeling study of the relative roles of tropical and extratropical SST anomalies in the variability of the global atmosphere-ocean system. Journal of Climate, 7(7): 1184–1207

Lau N C, Nath M J. 1996. The role of the "atmospheric bridge" in linking tropical Pacific ENSO events to extratropical SST anomalies. Journal of Climate, 9(9): 2036–2057, doi: 10.1175/1520-0442(1996)009<2036:TROTBI>2.0.CO;2

Li Gang, Chen Jiepeng, Wang Xin, et al. 2017. Modulation of Pacific Decadal Oscillation on the relationship of El Niño with southern China rainfall during early boreal winter. Atmospheric Science Letters, 18(8): 336–341, doi: 10.1002/asl.761

Lienert F. 2011. Simulation and Prediction of North Pacific Sea Surface Temperature. Victoria: University of Victoria.

Mantua N J, Hare S R, Zhang Yuan, et al. 1997. A Pacific interdecadal climate oscillation with impacts on salmon production. Bulletin of the American Meteorological Society, 78(6): 1069–1079, doi: 10.1175/1520-0477(1997)078<1069:APICOW>2.0.CO;2

Namias J, Born R M. 1970. Temporal coherence in North Pacific sea-surface temperature patterns. Journal of Geophysical Research, 75(30): 5952–5955, doi: 10.1029/JC075i030p05952

Overland J E, Alheit J, Bakun A, et al. 2010. Climate controls on marine ecosystems and fish populations. Journal of Marine Systems, 79(3-4): 305–315, doi: 10.1016/j.jmarsys.2008.12.009

Qiao Fangli, Song Zhenya, Bao Ying, et al. 2013. Development and evaluation of an Earth System Model with surface gravity waves. Journal of Geophysical Research Oceans, 118(9): 4514–4524, doi: 10.1002/jgrc.20327

Qiao F L, Yuan Y L, Ezer T, et al. 2010. A three-dimensional surface wave-ocean circulation coupled model and its initial testing. Ocean Dynamics, 60(5): 1339–1355, doi: 10.1007/s10236-010-0326-y

Qiao Fangli, Yuan Yeli, Yang Yongzeng, et al. 2004. Wave-induced mixing in the upper ocean: Distribution and application to a global ocean circulation model. Geophysical Research Letters, 31(11): L11303

Ratheesh S, Sharma R, Basu S. 2012. Projection-based assimilation of satellite-derived surface data in an Indian ocean circulation model. Marine Geodesy, 35(2): 175–187, doi: 10.1080/01490419.2011.637855

Shu Qi, Qiao Fangli, Bao Ying, et al. 2015. Assessment of Arctic sea ice simulation by FIO-ESM based on data assimilation experiment. Haiyang Xuebao (in Chinese), 37(11): 33–40

Song Zhenya, Qiao Fangli, Lei Xiaoyan, et al. 2007. The establishment of an atmosphere-wave-ocean circulation coupled numerical model and its application in the North Pacific SST simulation. Journal of Hydrodynamics (in Chinese), 22(5): 543–548

Song Zhenya, Shu Qi, Bao Ying, et al. 2015. The prediction on the 2015/16 El Niño event from the perspective of FIO-ESM. Acta Oceanologica Sinica, 34(12): 67–71, doi: 10.1007/s13131-015-0787-4

Wang Xin, Wang Dongxiao, Zhou Wen. 2009. Decadal variability of twentieth-century El Niño and La Niña occurrence from observations and IPCC AR4 coupled models. Geophysical Research Letters, 36(11): L11701, doi: 10.1029/2009GL037929

Wen Caihong, Xue Yan, Kumar A. 2012. Seasonal prediction of North Pacific SSTs and PDO in the NCEP CFS hindcasts. Journal of Climate, 25(17): 5689–5710, doi: 10.1175/JCLI-D-11-00556.1

Xing Wen, Wang Bin, Yim S Y. 2016. Long-lead seasonal prediction of China summer rainfall using an EOF-PLS regression-based methodology. Journal of Climate, 29(5): 1783–1796, doi: 10.1175/JCLI-D-15-0016.1

Yeh S W, Wang Xin, Wang Chuanzai, et al. 2015. On the relationship between the North Pacific climate variability and the central Pacific El Niño. Journal of Climate, 28(2): 663–677, doi:

10.1175/JCLI-D-14-00137.1

Yin Xunqiang. 2015. Development of assimilation module for ensemble adjustment Kalman filter and its applications in ocean and climate system models (in Chinese) [dissertation]. Qingdao: Ocean University of China

Yin Xunqiang, Qiao Fangli, Yang Yongzeng, et al. 2010. An ensemble adjustment Kalman filter study for Argo data. Chinese Journal of Oceanology and Limnology, 28(3): 626–635, doi: 10.1007/s00343-010-9017-2

Yu Jinyi, Wang Xin, Yang Song, et al. 2017. The changing El Niño–Southern Oscillation and associated climate extremes. In: Wang S Y S, Yoon J H, Fuck C C, et al., eds. Climate Extremes: Patterns and Mechanisms. Hoboken, NJ: AGU Geophysical Monograph Series, 226: 3–38

Yuan Y, Qiao F, Hua F, et al. 1999. The development of a coastal circulation numerical model: 1. Wave-induced mixing and wave-current interaction. Chinese Journal of Hydrodynamics (in Chinese), 14: 1–8

Zhang Ying, Zhu Jieshun, Li Zhongxian, et al. 2017. Sea surface temperature predictions using a multi-ocean analysis ensemble scheme. Climate Dynamics, 49(3): 1049–1059, doi: 10.1007/s00382-016-3100-0

Zhao Xia, Li Jianping, Zhang Wenjun. 2012. Summer persistence barrier of sea surface temperature anomalies in the central western north pacific. Advances in Atmospheric Sciences, 29(6): 1159–1173, doi: 10.1007/s00376-012-1253-2

Zhou Wen, Li Chongyin, Wang Xin. 2007. Possible connection between Pacific Oceanic interdecadal pathway and east Asian winter monsoon. Geophysical Research Letters, 34(1): L01701

Zhu Jieshun, Kumar A, Wang Hui, et al. 2015. Sea surface temperature predictions in NCEP CFSv2 using a simple ocean initialization scheme. Monthly Weather Review, 143(8): 3176–3191, doi: 10.1175/MWR-D-14-00297.1